Electronic Supplementary Information

The Nanomechanical Signature of in Liver Cancer Tissues and Its Molecular Origin

Mengxin Tian[#a], Yiran Li[#c], Weiren Liu[#a], Lei Jin[a], Xifei Jiang[a], Xinyan Wang[d], Zhenbin Ding[a], Yuanfei Peng[a], Jian Zhou[a,b], Jia Fan[a,b], Yi Cao[*c], Wei Wang[c], Yinghong Shi[*a]

Author Affiliations:

a. Department of Liver Surgery, Liver Cancer Institute, Zhongshan Hospital, Fudan University; Key Laboratory of Carcinogenesis and Cancer Invasion of Ministry of Education, Shanghai, China.

b. Institutes of Biomedical Sciences, Fudan University, Shanghai, People's Republic of China.

c. Collaborative Innovation Center of Advanced Microstructures, National Laboratory of Solid State Microstructure and Department of Physics, Nanjing 210093, P.R. China.

d. National Center for Protein Science Shanghai (NCPSS), Institute of Biochemistry and Cell Biology (SIBCB), Shanghai Institutes for Biological Sciences (SIBS), Chinese Academy of Sciences (CAS), Shanghai, China.

#. These authors contributed equally to this work

*Corresponding author

Dr. Ying-Hong Shi

Address: Department of Liver Surgery, Liver Cancer Institute, Zhongshan Hospital, Fudan University, 180 FengLin Road, Shanghai, 200032, China.

Tel.: (+86)-21-64041990-3233; fax: (+86)-21-64037181.

E-mail: shi.yinghong@zs-hospital.sh.cn

Or to Dr. Yi Cao

Address: Department of Physics, Nanjing University, 22 Hankou Road, Nanjing, Jiangsu, 210093, China.

Tel.: (+86)-25-8368 8960; fax: (+86)-25-83595535.

E-mail: caoyi@nju.edu.cn

Supplementary Tables.

Table S1. Nanomechanical results (Young's modulus *E*, mean ± SD) of different patients associated with pathology diagnosis.

Case	Age/gender	AFM elasticity values[kPa]				Pathology
		Peak1	Peak2	Peak3	Peak4	
1	37/female	1.08 ± 1.09				Healthy
2	62/female	1.16 ± 0.20				Healthy
3	72/male	1.26 ± 1.12				Healthy
4	29/female	1.46 ± 0.60				Healthy
5	38/female	0.91 ± 0.44				Healthy
6	67/female	1.16 ± 0.42				Healthy
7	73/female	1.32 ± 0.49				Healthy
8	51/male	1.15 ± 0.51	1.90 ± 0.60			Liver cirrhosis
9	77/male	1.25 ± 0.69	5.15 ± 1.11			Liver cirrhosis
10	77/male	0.95 ± 0.36	1.63 ± 0.38			Liver cirrhosis
11	59/male	0.89 ± 0.35	2.10 ± 0.33	3.31 ± 0.31		Liver cirrhosis
12	66/male	1.10 ± 0.20	1.85 ± 0.29			Liver cirrhosis
13	52/male	1.10 ± 0.91	2.30 ± 1.55			Liver cirrhosis

14	50/male	0.69 ± 0.23	2.08 ± 0.73			Liver cirrhosis
15	64/male	1.22 ± 0.60	1.92 ± 0.47	3.38 ± 1.02		Liver cirrhosis
16	46/male	1.12 ± 0.36	2.33 ± 0.40			Liver cirrhosis
17	63/male	0.96 ± 0.76	1.94 ± 0.85	3.50 ± 2.50		Liver cirrhosis
18	61/male	0.80 ± 0.51	2.77 ± 0.99	6.80 ± 2.36	12.28 ± 1.05	Liver cirrhosis
19	59/male	1.65 ± 0.47	2.75 ± 0.49			Liver cirrhosis
20	42/male	1.45 ± 0.72	2.69 ± 0.32	4.29 ± 0.84		Liver cirrhosis
21	64/male	0.60 ±0.30	1.50 ± 0.72	3.20 ± 0.41		Liver cirrhosis
22	67/female	0.63 ± 0.32	1.36 ± 0.39			HCC
23	51/male	0.60 ± 0.59	1.30 ± 0.45			HCC
24	77/male	1.05 ± 0.45	2.12 ± 1.72			HCC
25	77/male	0.95 ± 0.32	3.05 ± 0.47	6.50 ± 2.5		HCC
26	59/male	0.62 ± 0.27				HCC
27	66/male	0.42 ± 0.17	1.34 ± 0.64			HCC
28	52/male	0.80 ± 0.40	1.60 ± 0.50			HCC
29	59/male	0.56 ± 0.58	4.20 ± 2.58			HCC
30	64/male	0.40 ± 0.40	1.20 ± 0.43			HCC
31	63/male	0.30 ± 0.99	2.30 ± 1.55			HCC

32	73/female	0.47 ± 0.31	1.30 ± 0.36			HCC
33	46/male	0.60 ± 0.27	2.28 ± 0.68			HCC
34	61/male	0.15 ± 0.13	1.96 ± 0.57			HCC
35	50/male	0.29 ± 0.16				Recurrent HCC
36	64/male	0.58 ± 0.37				Recurrent HCC
37	90/male	0.65 ± 0.13	2.26 ± 0.60			Colon cancer
38	67/male	0.65 ± 0.57	1.74 ± 0.60	2.93 ± 0.80	13.00 ± 5.81	Esophageal cancer
39	28/male	0.51 ± 0.11	1.10 ± 0.78	6.51± 0.57	17.35 ± 1.58	Clear cell renal cell carcinoma
40	35/male	0.33 ± 0.14				Papillary renal cell carcinoma

mean ± SD [kPa]					
Normal		HCC (Metastatic and invasive potential)			
		Low		High	
L02	0.83 ± 0.51	SMMC7721	0.98 ± 0.84	MHCC97L	0.32 ± 0.58
		Huh7	1.02 ± 2.69	HCCM97H	0.51 ± 0.36
				HCCLM3	0.22 ± 0.18

Table S2. Mechanical properties of the HCC cell lines.

Table S3. Univariate analyses of prognostic factors associated with OS and TTR (n=751)

Variables	OS		TTR	
	HR(95% CI)	P	HR(95% CI)	P
Univariate analyses†				
Sex (male vs. female)	0.817 (0.586~1.138)	0.231	1.074（0.805~1.432）	0.629
Age, years (>50 vs. ≤50)	1.052 (0.822~1.346)	0.689	1.186（0.965~1.458）	0.105
HBsAg (positive vs. negative)	1.164 (0.839~1.616)	0.363	1.310（0.982~1.748）	0.066
TB, μmol/L (>17 vs. ≤17)	0.819 (0.627~1.070)	0.143	0.944（0.761~1.171）	0.600
ALT, U/L（>40 vs. ≤40)	1.116 (0.868~1.434)	0.391	1.064（0.864~1.311）	0.556
γ-GT, U/L (≤54 vs. >54)	1.002 (1.001~1.003)	**0.000**	1.001（1.000~1.002）	**0.004**
ALB, g/dl（≤3.5 vs. >3.5)	0.525 (0.344~0.801)	**0.003**	0.740（0.506~1.081）	0.119
AFP, ng/ml (>20 vs. ≤20)	1.424 (1.096~1.851)	**0.008**	1.391（1.122~1.724）	**0.003**
Liver cirrhosis (yes vs. no)	1.168（0.830~1.643）	0.374	1.378（1.025~1.853）	**0.034**
Tumor differentiation (III-IV vs. I-II)	1.446（1.118~1.870）	**0.005**	1.391（1.121~1.724）	**0.003**
Tumor encapsulation (none vs. complete)	1.198（0.945~1.519）	0.135	1.181（0.969~1.439）	0.099

Tumor size, cm (>5 vs. ≤5)	2.080（1.628~2.657）	**0.000**	1.722（1.401~2.117）	**0.000**
Vascular invasion (yes vs. no)	1.462（1.140~1.870）	**0.003**	1.544（1.252~1.903）	**0.000**
TNM stage (I vs. II III)	1.243（0.735~2.101）	0.417	1.263（0.784~2.036）	**0.338**
Tumor number (multiple vs. single)	1.260（0.855~1.858）	0.242	1.143（0.791~1.651）	0.478
mDia1 in tumor (low vs. high)	0.772（0.601~0.991）	**0.042**	0.960（0.774~1.192）	0.714

Abbreviations: TTR time to recurrence; OS, overall survival; AFP:α-fetoprotein; γ-GT, γ-glutamyl transferase; TNM, tumor-nodes-metastasis; HR, hazard ratio; CI, confidential interval; NA, not adopted. Boldface type indicates significant values. †Cox proportional hazards regression.

Table S4. The associated primer sequences.

Name(Human)	Primer	Sequence(5'-3')
mDia1	Forward	GGAGTTACGATAGCCGGAACA
	Reverse	CTTCTGTCTCCAACATGGTCTTG
RhoA	Forward	AGCCTGTGGAAAGACATGCTT
	Reverse	TCAAACACTGTGGGCACATAC
RhoB	Forward	ATCCCCGAGAAGTGGGTCC
	Reverse	CGAGGTAGTCGTAGGCTTGGA
RhoC	Forward	GGAGGTCTACGTCCCTACTGT
	Reverse	CGCAGTCGATCATAGTCTTCC
ROCK1	Forward	AAGTGAGGTTAGGGCGAAATG
	Reverse	AAGGTAGTTGATTGCCAACGAA
GADPH	Forward	AAGGTGAAGGTCGGAGTCAAC
	Reverse	GGGGTCATTGATGGCAACAATA

Supplementary Figures.

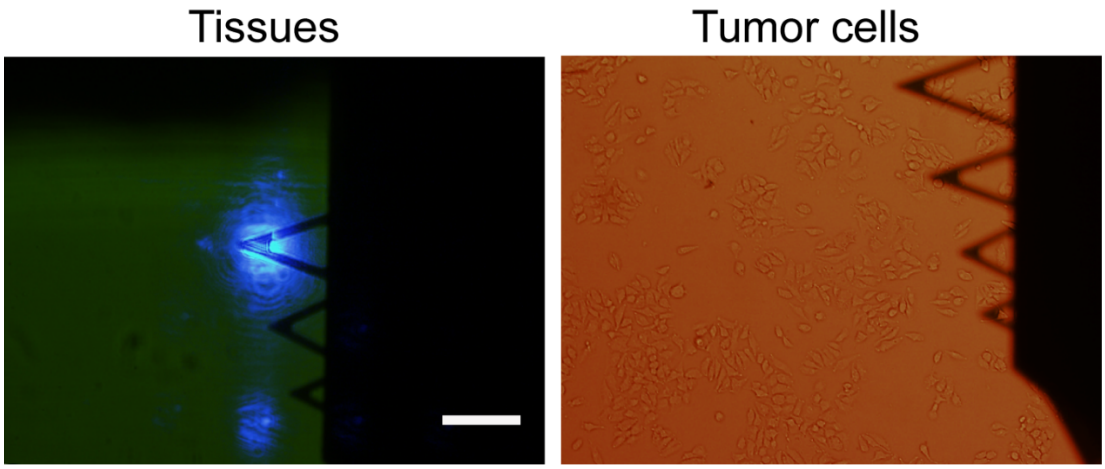

Figure S1 Measuring the mechanical properties of tissues (left) and cells (right) using IT-AFM. Scale bar, 200 μm.

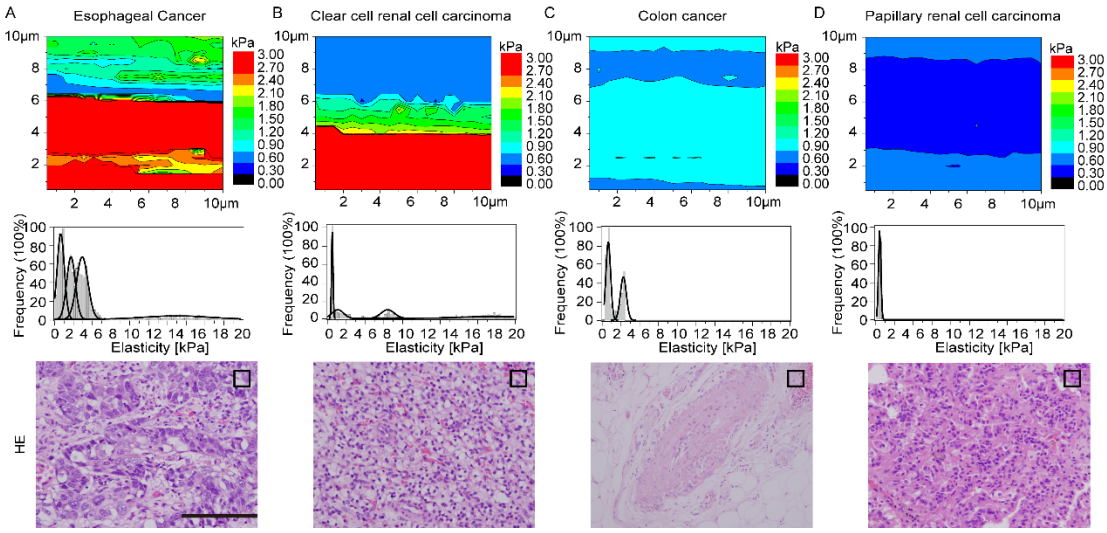

Figure S2 The downshift of LSP is a common feature shared by many kinds of cancer. A-D, Mechanical features of esophageal cancer, clear cell renal cell carcinoma, colon cancer and papillary renal cell carcinoma, respectively. Top panel: Representative elasticity maps (10 μm × 10 μm, 100 pixels) of different tissue samples. Middle panel: Distribution of the Young's moduli for each sample. Bottom panel: HE staining for each sample. A dark square (10 μm × 10 μm, 100 pixels) represents the size of elasticity map in Tri. Masson staining. Scalebar: 50 μm.

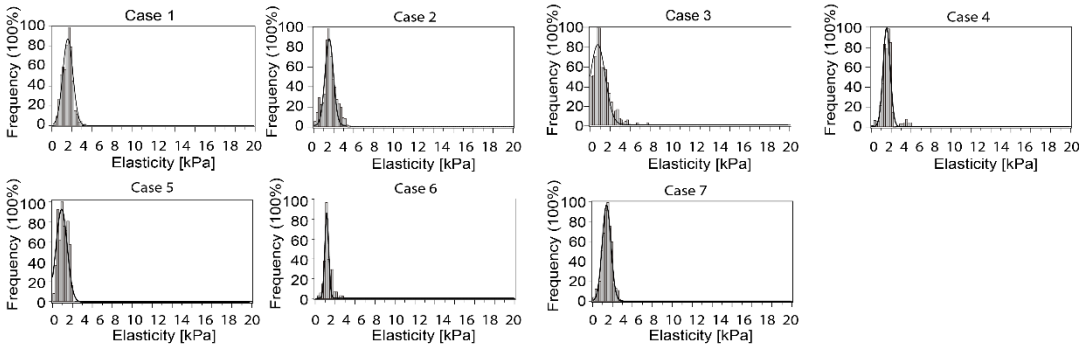

Figure S3 The elasticity distribution of normal liver tissues measured by IT-AFM.

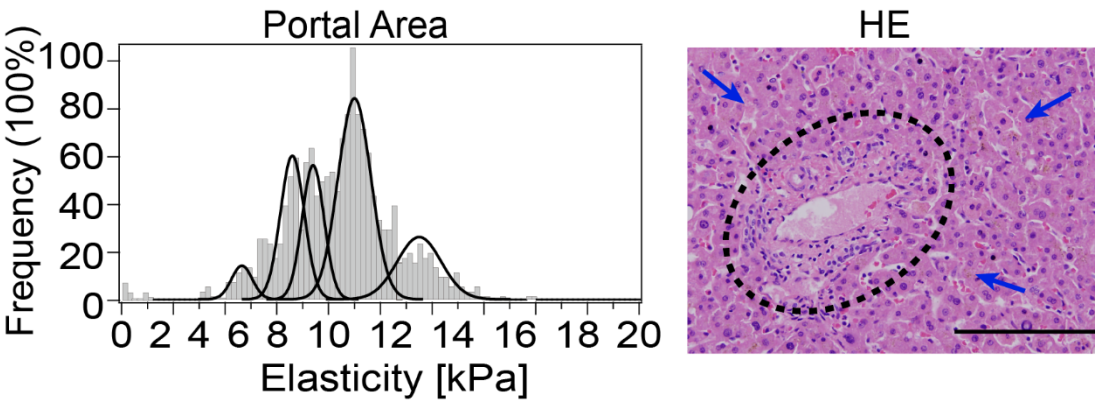

Figure S4 The mechanical properties of the portal area. (left) The distribution of the Young's moduli of the portal area measured by IT-AFM. (right) HE image of the portal area. The circled area corresponds to the portal area and the arrows indicate the normal tissues. Scale bar, 50 μm.

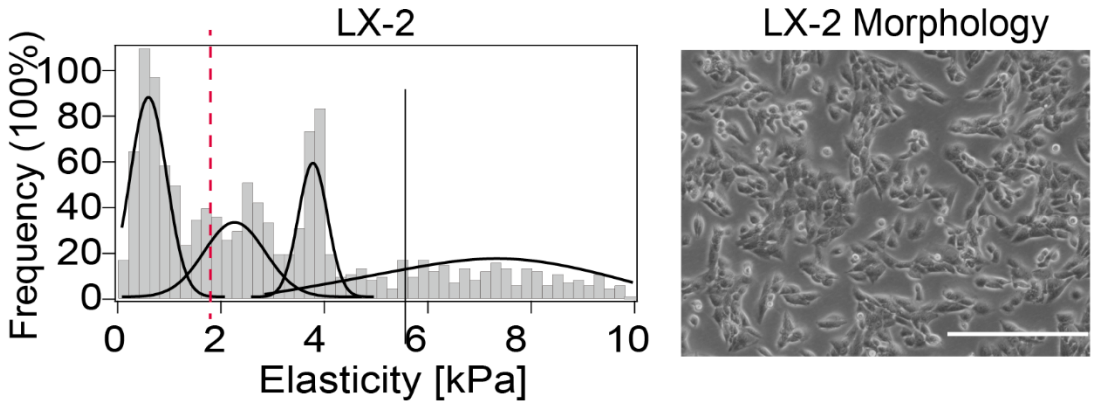

Figure S5 The mechanical properties of in vitro cultured LX-2 cells measured by IT-AFM. (A) The distribution of the Young's moduli of the portal area measured by IT-AFM. (B) A representative optical image of LX-2 cells cultured on a 6-well petri dish. Scale bar, 50 μm.

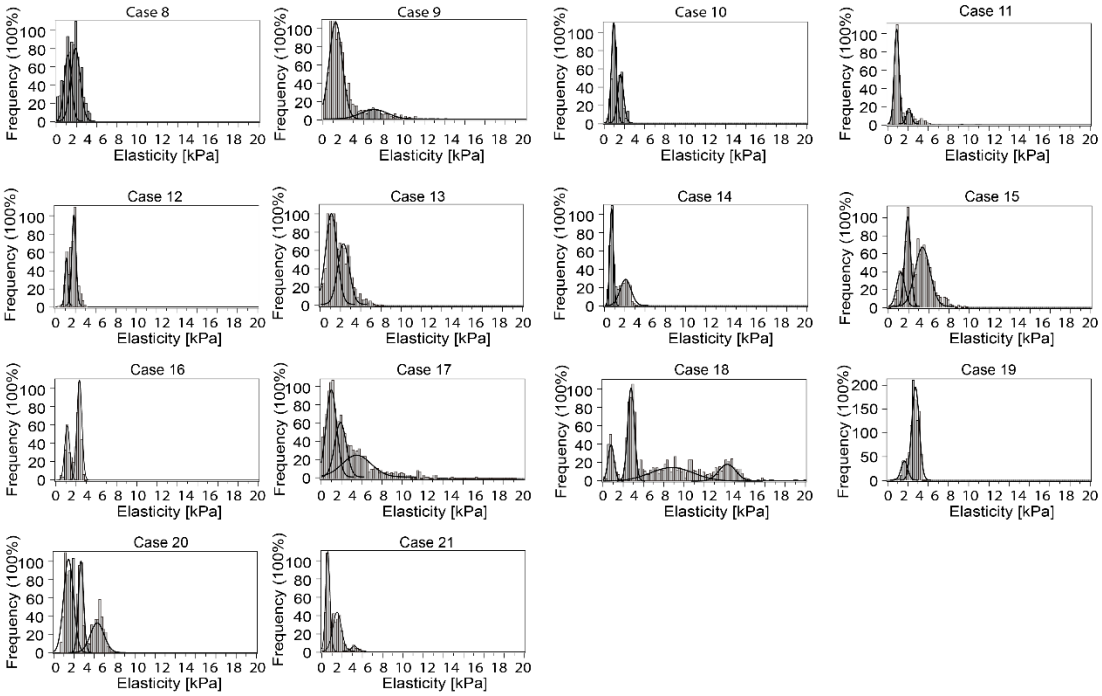

Figure S6 Elastic histograms showed the elasticity distributions for liver samples with liver cirrhosis.

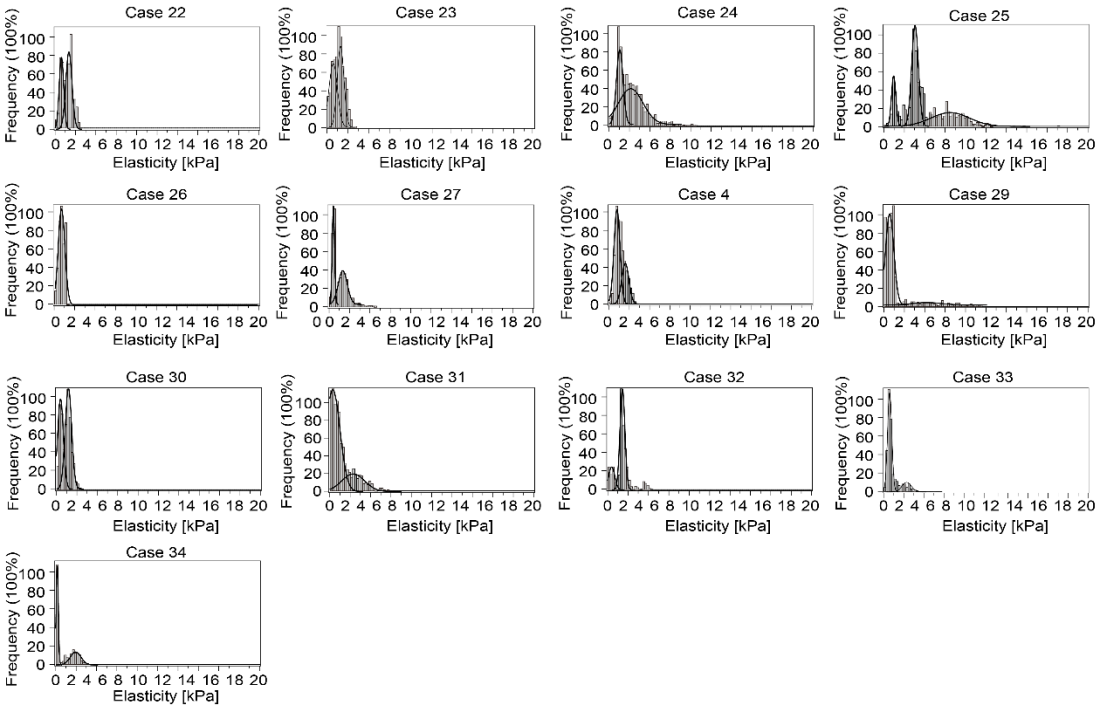

Figure S7 Post-AFM analysis showed the elasticity distributions for human HCC samples tested.

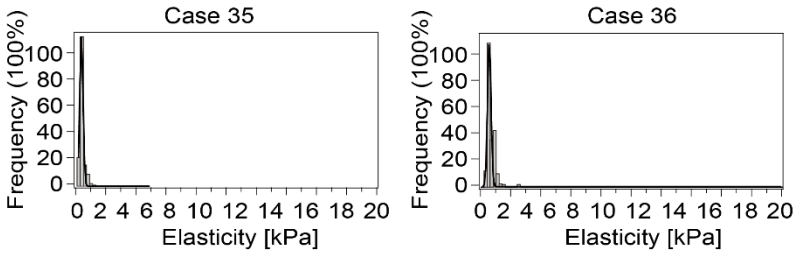

Figure S8 The elasticity distribution of recurrent HCC.

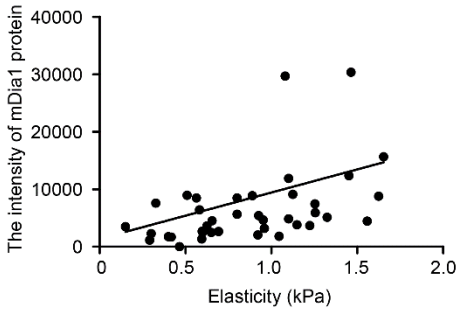

Figure S9 The scatter plot between mDia1 expression level and its relevant elasticity in detected liver tissues.

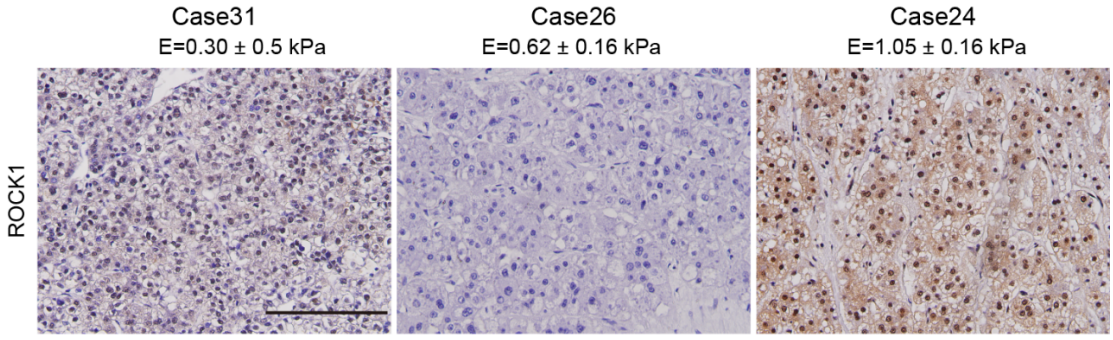

Figure S10 ROCK1 expression levels in different tissues with various elasticity. The stages of brown staining area represented different expression level. Scale bar, 50 μm.

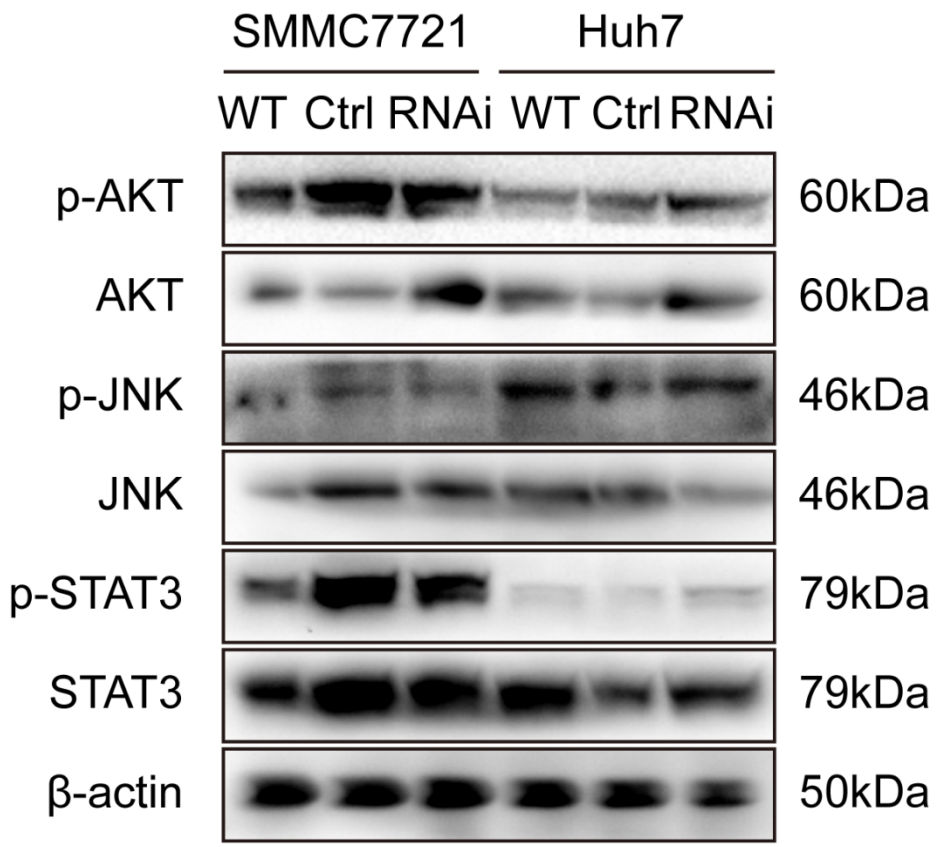

Figure S11 mDia1 didn't induced phosphorylation of Akt, JNK and STAT3 in HCC cells.

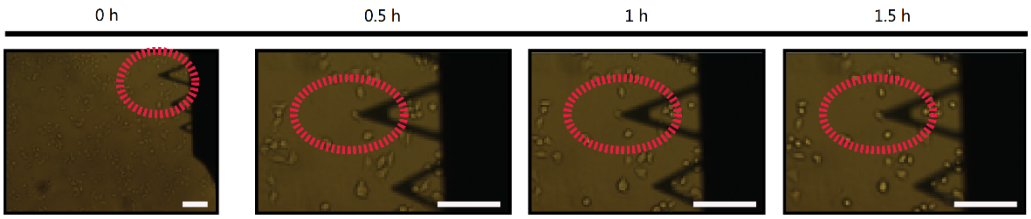

Figure S12 Optical images for cell survival test. We carried on an experiments on the same cell and the experimental reference is the same. We took optical images after every half hour. From the optical images, we can see the cell remain the same shape and adhered to the petri dish after the indentation measurement. The dead cells typically cannot remain attached on the petri dish and will go to the suspension. The error bars in each image correspond to 200 μm.

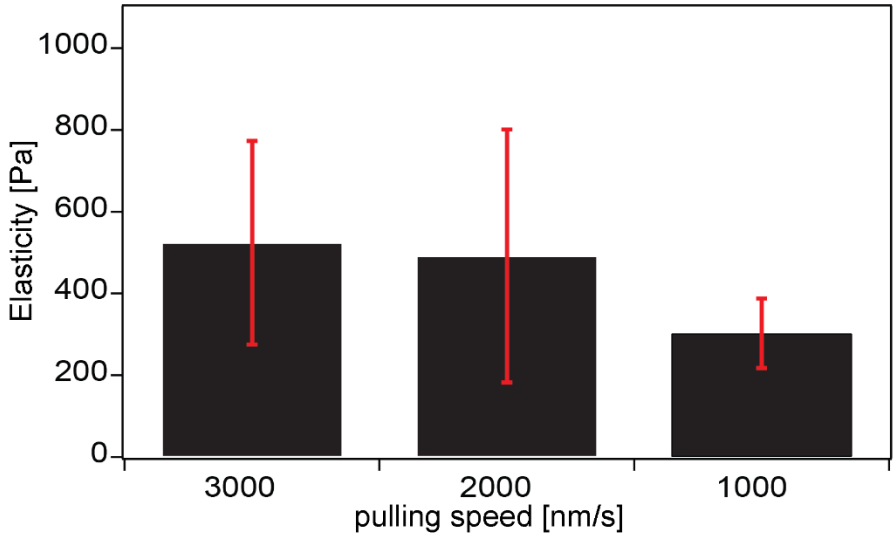

Figure S13 Loading rate dependent experiment. We found that lower the speed to 2 μm/s could lead to the decrease of the elasticity by 5%.

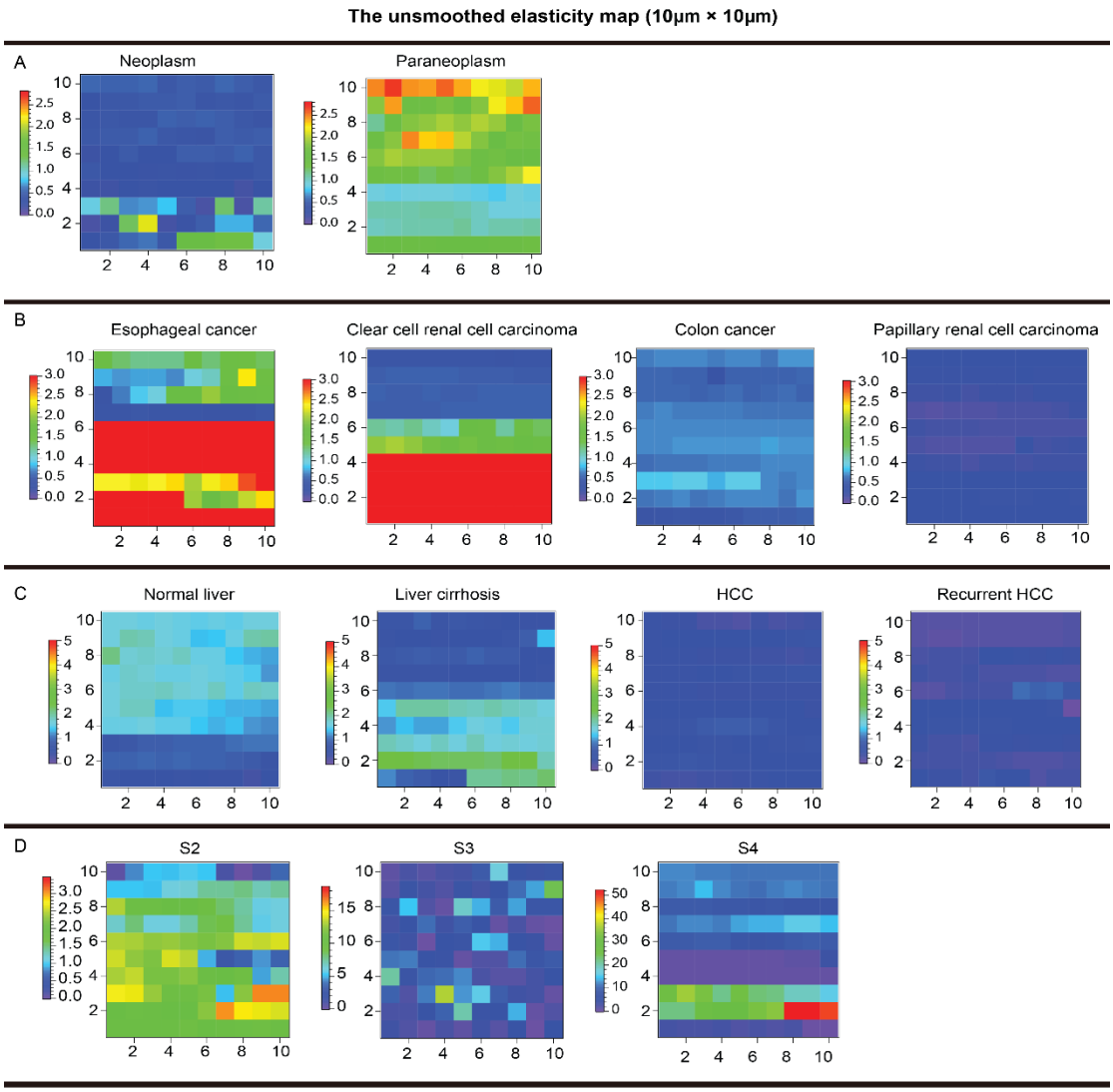

Figure S14 Unsmoothed data of elasticity map. In manuscript, we used a two-dimensional spline interpolation for better visual presentation of the data. To illustrate how smoothing procedure changes the results, we attached the unsmoothed data here. A correspond to the two elasticity map in Figure 1. B corresponds to the elasticity map in Figure S2. C corresponds to the elasticity map in Figure 2. D corresponds to the elasticity map in Figure 3.

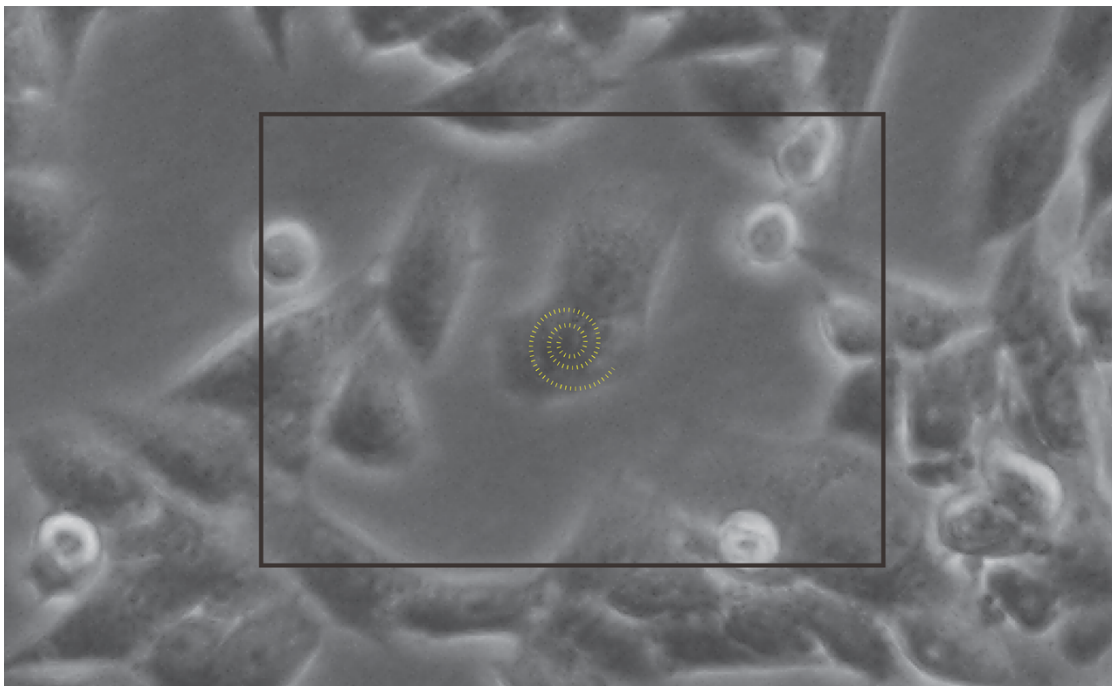

Figure S15 Test route on cell sample. We set a spiral pattern with rotation angle θ=45° and tested 100 spots on this route.